Scientia Iranica, Vol. 6, No. 2, pp 86–100

SCIENTIA
IRANICA

Failure Analysis of Laminated Composite Pinned Connections

G. Karami* and M.R. Sharifi-Jah[1]

In this paper, a progressive damage modeling method is employed to predict the failure of pinned joints made up of fiber reinforced composite laminates. The analysis is performed using finite element techniques. Two approaches towards analysis are implemented. One is based on linear modeling and the second one has been enhanced by nonlinearity of the material behavior. The failure load and mode are then predicted by means of a logical combination of suitable failure criteria and appropriate material property degradation rules. A computer code is developed which can be used to predict the maximum failure load, together with the failure mode of the laminated joints with different ply orientation material properties and geometries. Results of the method are compared with those of other experimental and theoretical methods for the same problems. Parametric studies were also performed to evaluate the effect of joint geometry and ply orientation on failure strength and mode.

INTRODUCTION

Among the major advantages of laminated composite structures over conventional metal structures are their comparatively high ratios of strength to weight and stiffness to weight. As a result, fiber reinforced composite materials have been widely applied in aircraft and spacecraft constructions. These applications require joining composite laminates either to other composites or to metals. The joints which are formed using mechanical fasteners often fail at the joint areas. Hence, suitable methods must be implemented to determine the failure strength of such fastened joints. Knowledge of failure strength would help in selecting the appropriate joint size and type in a given application. There has been extensive research work on the analysis of pinned joints. The following literature review is confined to those where the finite elements technique has been used as a tool of analysis. Waszczak and Cruse [1] implemented a finite element analysis in conjunction with a distorsional energy failure criterion for predicting failure mechanism and ultimate load. Humphris [2] investigated the strength of a laminated composite structure by using Tsai-Hill failure criterion to study the failure trend. Soni [3] circumvented this by delaying the application of the quadratic failure criterion until all plies had reached failure. Work by Tsiang and Mandell [4], Conti [5] and Serabian and Oplinger [6] used Tsai-Hill criterion, however, they examined only failure initiation. In order to predict failure modes, models have been developed which incorporate the concept of progressive damage modeling [7-9]. A complete two-dimensional study has been carried out by Lessard [8] and Lessard and Shokrieh [9], in which they have investigated the damage behavior of pin-loaded composite plates and have developed a damage progression model capable of predicting net-tension, shear-out and bearing failure modes.

The aim of this paper is to present a finite element analysis in conjunction with a progressive damage modeling of laminated pinned joints. Different failure criterion together with both linear and nonlinear material behavior modeling are to be employed and the results are compared with those from the experiments. Although fiber buckling and delamination is a possibility where the fibers go under severe compression loads, this phenomenon is not to be taken into consideration in the forthcoming analysis.

*. *Corresponding Author, Department of Mechanical Engineering, School of Engineering, Shiraz University, Shiraz, P.O. Box 71345-1584, I.R. Iran.*

1. *Department of Mechanical Engineering, School of Engineering, Shiraz University, Shiraz, P.O. Box 71345-1584, I.R. Iran.*

A LAMINATED PINNED JOINT

Consider a plate (length L, width W, thickness H) made of N fiber reinforced unidirectional plies, as shown in Figure 1. The ply orientations are arbitrary but must be symmetric with respect to the plane. Perfect bonding between each ply is assumed. A single hole of diameter D is located along the center line of the plate and a rigid pin is inserted into the hole.

Under tensile loads, mechanically fastened joints generally fail in three basic modes referred to as net-tension, shear-out and bearing (in addition, a combination of these three mechanisms may occur). Typical damage due to each mechanism is shown in Figure 2.

In order to determine the state of propagation of damage at any load level and the extent of the contact region between the rig pin and the plate in the hole region, a progressive damage modeling method is used to analyze the pinned joint problem. This method consists of three major parts: the primary stress analysis, checking for the failure and degradation of material properties in the damaged regions (an iterative procedure); linear and nonlinear analyses and the respective failure criterion and degradation in each type of analysis.

A computer code has been developed which can be conveniently used for the analysis of laminated composites containing pin loaded holes.

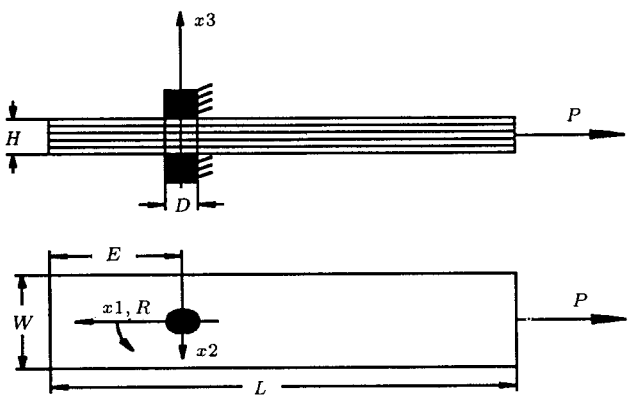

Figure 1. Geometry of the laminate containing a pin-loaded hole.

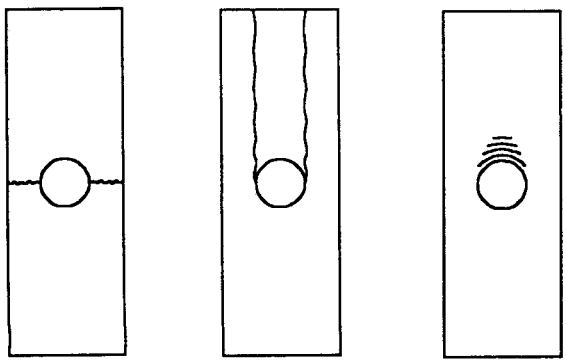

Figure 2. Typical failure mechanisms for the pinned joint configuration.

THE LINEAR 2-D MODELING

Stress Analysis

A closed form solution for the stress analysis of composites, in particular the pin loaded joints, cannot be found in the literature. Furthermore, because of high nonlinear nature after failure due to the change in material properties of damaged regions, the approximate analytical solutions are no longer valid. For these reasons and the nature of progressive damage modeling, the finite element technique is a suitable tool for the analysis of such cases. Two-dimensional approximation modelings have been commonly used, mainly due to the computing efficiency of two-dimensional finite element modeling. In cases like the pinned/bolted joint, the two dimensional plane-stress approximation is quite valid and can provide useful results. However, in the joining configuration, where out-of-plane effects may play an essential role in the failure analysis, the two-dimensional analysis is insufficient.

Stress on the laminate is calculated on the basis of anisotropic theory of elasticity. Accordingly, the strain $\epsilon_{ij}(x, y)$ is assumed to be a function of the coordinates on the plane of the junction and cross thickness is considered to be constant. The general stress-strain relation for orthotropic material may be expressed as:

$$\{\sigma\} = [C]\{\epsilon\} \ , \tag{1}$$

where the stiffness matrix $[C]$ is in the form of:

$$[C] = \begin{bmatrix} C_{11} & C_{12} & C_{16} \\ C_{21} & C_{22} & C_{26} \\ C_{61} & C_{62} & C_{66} \end{bmatrix} \ . \tag{2}$$

If the plate is made of N layers, then the equivalent stiffness may be determined according to:

$$C_{ij}^n = \sum_{p=1}^{N} \frac{h^p}{H} (C_{ij}^p)^n \ , \tag{3}$$

where h and H are the thickness of pth ply and the thickness of the plate, respectively. $(C_{ij}^p)^n$ is the transformed reduced stiffness matrix for pth ply at nth increment. (C_{ij}^p) is transformed reduced stiffness matrix of laminate at nth increment. By employing the equilibrium equations together with the kinematical relations in conjunction with the constitutive equations described above, the governing equations may be derived. If this equation is multiplied by the chosen shape

functions integrated over the element domain and the divergence theorem is applied one can derive the usual weak formulation in matrix form as:

$$\begin{bmatrix} K_{ij}^{11} & K_{ij}^{12} \\ K_{ij}^{21} & K_{ij}^{22} \end{bmatrix} \begin{Bmatrix} u_j \\ v_j \end{Bmatrix} = \begin{Bmatrix} F_i \\ F_i \end{Bmatrix} , \tag{4}$$

where,

$$K_{ij}^{11} = \int_{\Omega^e} h\left(C_{11}\frac{\partial N_i}{\partial x}\frac{\partial N_j}{\partial x} + C_{16}\left[\frac{\partial N_i}{\partial x}\frac{\partial N_j}{\partial y} + \frac{\partial N_i}{\partial y}\frac{\partial N_j}{\partial x}\right] + C_{66}\frac{\partial N_i}{\partial y}\frac{\partial N_j}{\partial y}\right) d\Omega^e ,$$

$$K_{ij}^{12} = \int_{\Omega^e} h\left(C_{12}\frac{\partial N_i}{\partial x}\frac{\partial N_j}{\partial y} + C_{16}\frac{\partial N_i}{\partial x}\frac{\partial N_j}{\partial x} + C_{26}\frac{\partial N_i}{\partial y}\frac{\partial N_j}{\partial y} + C_{66}\frac{\partial N_i}{\partial y}\frac{\partial N_j}{\partial x}\right) d\Omega^e ,$$

$$K_{ij}^{21} = K_{ij}^{12} ,$$

$$K_{ij}^{22} = \int_{\Omega^e} h\left(C_{66}\frac{\partial N_i}{\partial x}\frac{\partial N_j}{\partial x} + C_{22}\frac{\partial N_i}{\partial y}\frac{\partial N_j}{\partial y} + C_{26}\left[\frac{\partial N_i}{\partial x}\frac{\partial N_j}{\partial y} + \frac{\partial N_i}{\partial y}\frac{\partial N_j}{\partial x}\right]\right) d\Omega^e ,$$

and:

$$F_i^1 = \oint_{\Gamma^e} hN_i t_x d\Gamma^e , \qquad F_i^2 = \oint_{\Gamma^e} hN_i t_y d\Gamma^e .$$

Note that N_i denote the shape functions and Ω_e and Γ_e are the domain and boundary of the eth element. To perform the calculations, the problem illustrated in Figure 1 was discretized into a number of linear isoparametric quadrilateral elements.

FAILURE CRITERION

There are numerous failure criteria for composite materials [10] as a direct result of the complex nature of observed failure phenomena. When examining these failure criteria, it is essential to keep in mind that these criteria are only useful if they can be incorporated into a progressive damage analysis, which usually means that they must be compatible with a finite element formulation. Hashin [11] failure criteria are polynomial failure criteria similar to the quadratic failure envelope except that in the Hashin formulation there are distinct polynomials corresponding to the different failure modes. Thus, Hashin type criteria combine the advantages of accuracy found in the polynomial criteria and the ability to distinguish failure mode found in the maximum stress criteria. However his criteria do not cover all the failure modes and in his matrix compressive failure mode formulation determining transverse shear strength is difficult. To resolve these difficulties, Chang and Lessard [12] and Lessard et al. [13] have completed Hashin criteria. This makes the combined failure criteria ideal for use in finite element models, especially when adapted to progressive damage models. For the composite laminated joints, the failure is checked here at each increment of loading for the following failure modes:

1. Matrix failure,
2. Fiber failure,
3. Matrix-fiber failure.

Of course, for each mode of failure the nature of the stress, whether it be tensile, compressive or shear, will make a difference.

Assuming x and y to be, respectively, the longitudinal and transverse directions of the plate under consideration, the following failure categories with their criterion may be explicitly defined.

Matrix Failure

Matrix Tensile Stress

According to Hashin failure criteria, cracking of the matrix material under tension would start once the stresses satisfy the relation,

$$\left(\frac{\sigma_y}{S_t^t}\right) + \left(\frac{\sigma_{xy}^2}{S_s^p}\right)^2 > 1 \quad \text{subjected to} \quad \sigma_y > 0, \tag{5}$$

where σ_y and σ_{xy} are the transverse tensile stress and shear stress in each layer, respectively. S_t^t is the transverse tensile strength and S_s^p is the ply shear strength.

Matrix Compressive Failure

Lessard and Shokrieh [9] proposed failure when the nature of stresses in the region is of the compression type once:

$$\left(\frac{\sigma_y}{S_c^t}\right) + \left(\frac{\sigma_{xy}^2}{S_s^p}\right)^2 > 1 \quad \text{subjected to} \quad \sigma_y < 0, \tag{6}$$

where σ_{xy} and S_s^p are defined as before, σ_y is the transverse compressive stress and S_c^t is the transverse compressive strength.

Fiber Failure

Fiber Tensile Failure

Hashin failure criteria have suggested the following relation for this mode of failure:

$$\left(\frac{\sigma_x}{S_t^\ell}\right) + \left(\frac{\sigma_{xy}^2}{S_s^p}\right)^2 > 1 \quad \text{with} \quad \sigma_x > 0, \tag{7}$$

where σ_x is the longitudinal fiber stress and S_t^ℓ is the

longitudinal tensile strength.

Fiber Compression (Bearing) Failure

In this mode of failure, Hashin states that it is not clear whether shear stress produces a weakening or strengthening effect on compressive strength in fiber direction. Consequently, the failure criterion is represented in the following simple maximum stress form:

$$\left(\frac{\sigma_x}{S_c^\ell}\right) > 1 \quad \text{subjected to} \quad \sigma_x < 0, \tag{8}$$

where S_c^ℓ is the fiber compression strength.

Fiber-Matrix Failure

This type of failure mostly occurs in shear mode, which is important for compression failure dominated by shear stresses. Hashin [11] proposed that the failure criteria in this mode take place once the following inequality is satisfied:

$$\left(\frac{\sigma_x}{S_t}\right) + \left(\frac{\sigma_{xy}^2}{S_s}\right)^2 > 1 \quad \text{subjected to} \quad \sigma_x > 0, \tag{9}$$

where S_t and S_s are defined as before.

Degradation

As soon as failure occurs, the material properties in the damaged region would be degraded. The degree of property loss strongly depends upon the failure mechanisms. In the following, a new material stiffness due to degradation is presented.

Matrix Degradation

If matrix failure in tension or compression is predicted in a layer of the laminate, only the transverse modulus and Poisson's ratio in the damaged area of the layer are reduced to zero. However, the longitudinal modulus and the shear properties of the layer are unchanged. The plane stress stiffness matrix is shown here both before and after application of the degradation rule.

$$\begin{bmatrix} \frac{E_x}{1-\nu_x\nu_y} & \frac{E_x\nu_y}{1-\nu_x\nu_y} & 0 \\ \frac{E_y\nu_x}{1-\nu_x\nu_y} & \frac{E_y}{1-\nu_x\nu_y} & 0 \\ 0 & 0 & G_{xy} \end{bmatrix} \Longrightarrow \begin{bmatrix} E_x & 0 & 0 \\ 0 & 0 & 0 \\ 0 & 0 & G_{xy} \end{bmatrix}, \tag{10}$$

where E_x and E_y are the fiber and matrix moduli, respectively, G_{xy} is the shear modulus and ν_x and ν_y are the Poisson's ratios associated with a single layer of composite material.

Fiber Degradation

In the damaged zone either under tensile or compressive loads for fiber breakage, both E_y and ν_y are reduced to zero, however, the longitudinal and shear moduli of the failed layer degenerate according to the Weibull distribution as follows:

$$\frac{\bar{E}_x}{E_x} = e^{-(\frac{A}{A_\circ})^\beta}, \quad \frac{\bar{G}_{xy}}{G_{xy}} = e^{-(\frac{A}{A_\circ})^\beta}, \tag{11}$$

where $\bar{E}_x$ and $\bar{G}_{xy}$ are the reduced tensile and shear moduli, respectively. A is the damage zone predicted by this mode, $A_\circ = \delta^2$ is the fiber failure interaction zone associated with the measured ply tensile strength X_t and β is the shape parameter of the Weibull distribution for the property degradation. δ can be estimated by the following expression [14]:

$$\delta = 2d\left(\frac{S_f}{4\tau_y}\right)^{\frac{\beta}{\beta+1}} \left[\frac{(\beta+1)L}{d}\right]^{\frac{1}{\beta+1}}, \tag{12}$$

where d is the diameter of the fibers, S_f is the average fiber strength, τ_y is the yielding stress of the matrix and L is the length of the fibers under consideration. For this catastrophic mode of failure, the plane stress stiffness matrix is shown here both before and after application of the degradation rule.

$$\begin{bmatrix} \frac{E_x}{1-\nu_x\nu_y} & \frac{E_x\nu_y}{1-\nu_x\nu_y} & 0 \\ \frac{E_y\nu_x}{1-\nu_x\nu_y} & \frac{E_y}{1-\nu_x\nu_y} & 0 \\ 0 & 0 & G_{xy} \end{bmatrix} \longrightarrow \begin{bmatrix} \bar{E}_x & 0 & 0 \\ 0 & 0 & 0 \\ 0 & 0 & \bar{G}_{xy} \end{bmatrix}. \tag{13}$$

Fiber-Matrix Degradation

For this mode of failure, the material loses its shear properties and Poisson's effect which are reduced to zero, however, the shear modulus of the failed layer would be degraded based on Equation 13. Therefore, for this mode of failure, the new material properties matrix is:

$$\begin{bmatrix} \frac{E_x}{1-\nu_x\nu_y} & \frac{E_x\nu_y}{1-\nu_x\nu_y} & 0 \\ \frac{E_y\nu_x}{1-\nu_x\nu_y} & \frac{E_y}{1-\nu_x\nu_y} & 0 \\ 0 & 0 & G_{xy} \end{bmatrix} \longrightarrow \begin{bmatrix} E_x & 0 & 0 \\ 0 & E_y & 0 \\ 0 & 0 & \bar{G}_{xy} \end{bmatrix}. \tag{14}$$

RESULTS OF THE LINEAR ANALYSIS

To assess the accuracy of the finite element code, problems with existing solutions were selected to be compared with the numerical solutions generated by the code. The first problem considered was an isotropic plate containing a pin loaded hole. As shown in Figure 3, the stresses calculated by the code are in good agreement with De Jong approximate solution [15]. The parameters used in numerical calculations are chosen as:

$$D = 0.3 \text{ in}, \ \frac{W}{D} = 0.5, \ \frac{E}{D} = 4.0, \ \frac{L}{D} = 14, \ P_b = \frac{P}{Dt}.$$

In the second problem, the stress distribution in an orthotropic plate with a finite width containing an open (unloaded) hole was calculated. The calculations were performed for a plate with symmetric laminate lay of up to $[0/90]_s$. An analytical solution for this problem

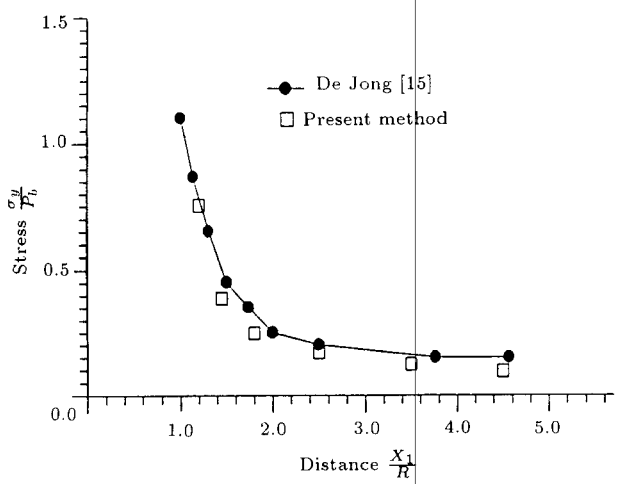

Figure 3. Stress σ_y along X-axis in an isotropic plate of finite width containing a loaded hole.

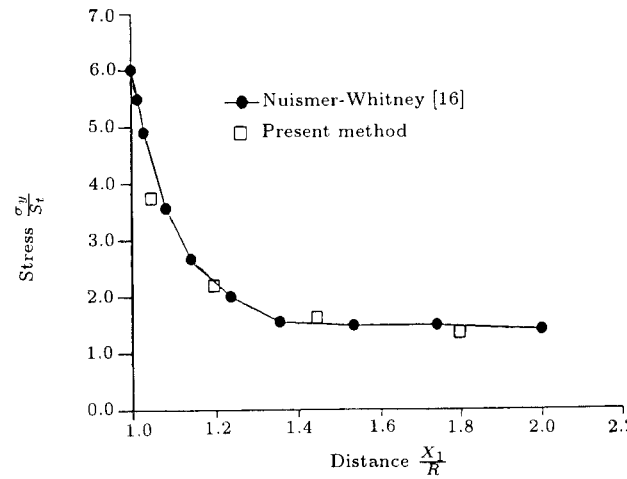

Figure 4. Stress σ_y along X-axis in an orthotropic finite plate $[0/90]_s$ containing a circular hole.

Table 1. Material properties for three graphite/epoxy materials.

		Materials		
		AS4/3501-6	***T*300/SP286**	***T*300/976**
E_x	(GPa)	156	130	150
E_y	(GPa)	13	8	8
E_s	(GPa)	7	5	5
ν_x	—	0.23	0.3	0.3
α	$(MPa)^{-3}$	2.4423×10^{-8}	—	3.64579×10^{-8}
S_t^ℓ	(MPa)	1517	1231	2308
S_c^ℓ	(MPa)	1593	1083	1585
S_t^t	(MPa)	46	50	43
S_c^t	(MPa)	253	193	842
S_s^p	(MPa)	107	50	115
β	(GPa)	7.6	6.6	7.6
δ	(mm^2)	0.355	—	0.3449

was provided previously by Nuismer and Whitney [16], who modified Lekhnitskii's earlier solution [17] for an infinite plate. The results given in Figure 4 show good agreement between the stresses calculated by the present code and those given by Nuismer and Whitney.

Comparison of the present results with the theoretical results given by Nuismer and Whitney [16] is demonstrated here. Parameters used in numerical calculations are:

Material: Graphite - Epoxy $T300/5208$

$E_1 = 1.4 \times 10^3$Ksi, $E_2 = 1.6 \times 10^3$Ksi,

$G_{12} = 0.77 \times 10^3$Ksi,

$\nu_{12} = 0.29$, $S_? = 0.333$Ksi,

$$D = 1\text{in}, \quad \frac{W}{D} = 0.3, \quad \frac{E}{D} = 4, \quad \frac{L}{D} = 14$$

Upon loading a laminated composite plate to final failure, the three main failure mechanisms become evident. For any particular case, the results can be generated by the proposed model through varying material properties, geometry or ply layout. Material properties for the cases studied are shown in Table 1.

To see how progressive damage modeling works, a sample case of a graphite-epoxy material ($T300/SP286$) with layout is chosen. The configuration and final failure mechanism are shown in Figures 5 and 6. The experimental failure load for this example

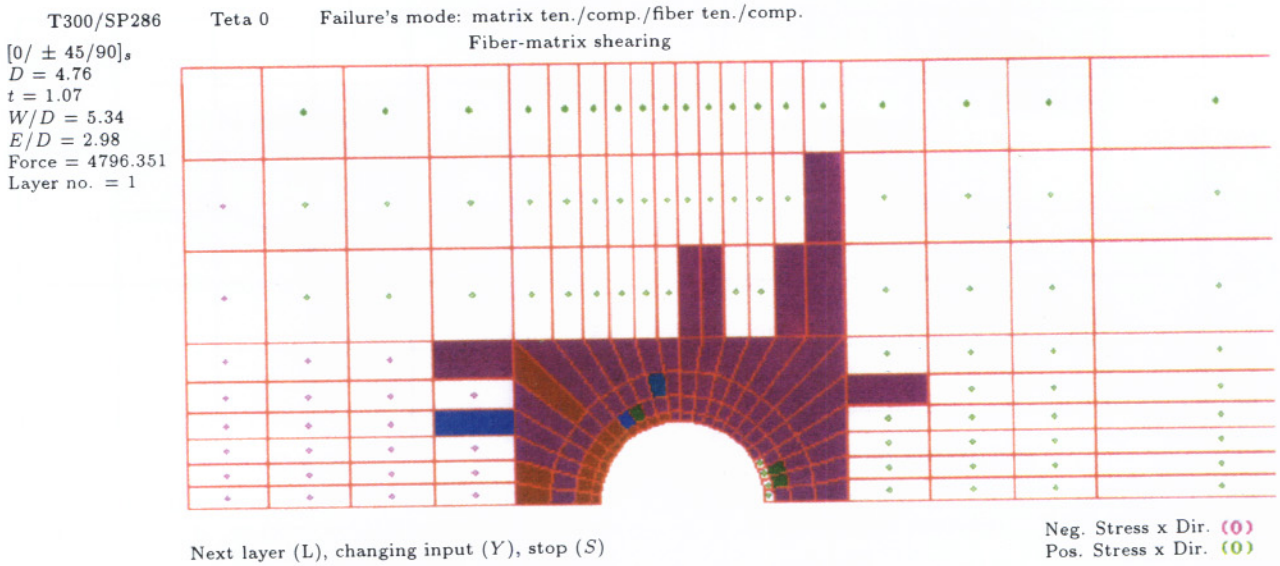

Figure 5. Predicted mechanism of failure for $[0/\pm 45/90]_s$, layer 1.

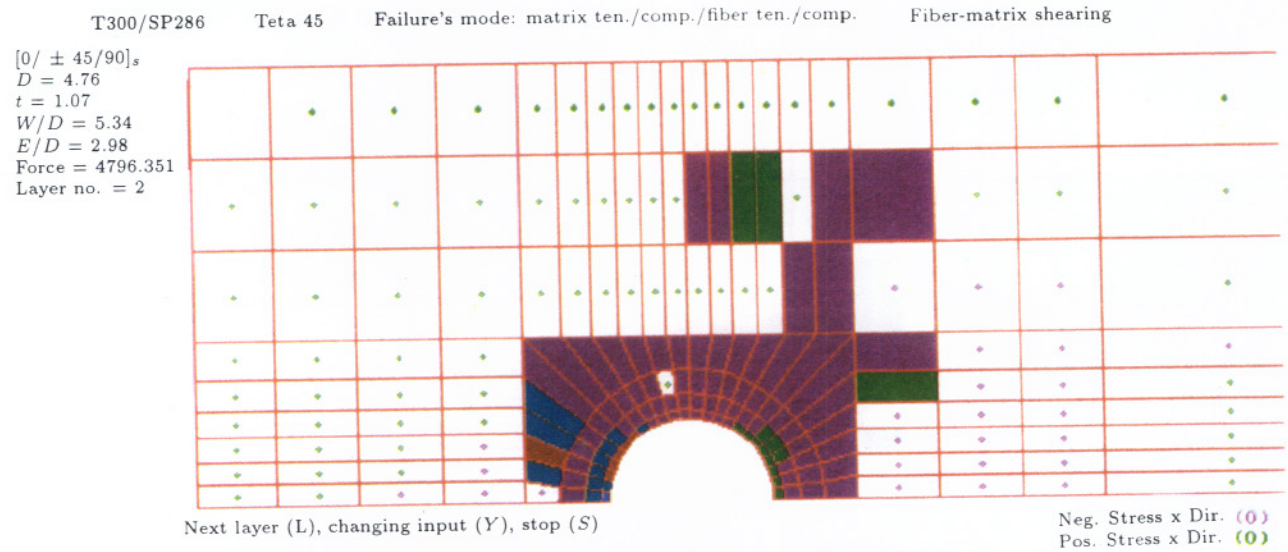

Figure 6. Predicted mechanism of failure for $[0/\pm 45/90]_s$, layer 2.

is reported 4982 N [9]. The failure load of 4796 N is predicted by the computer code which is 3.73% below the experimental failure load.

Parametric studies have been performed using the computer program for various materials, geometry and ply configurations. As an example of a parametric study, the following case is considered: using graphite epoxy material $T300/976$ (see Table 1 for material properties), with a cross ply laminate configuration, bearing strengths are compared for various geometries, as shown in Figures 7a and 7b.

The trends in the results are evident and make sense upon examination. In Figure 7a, there is a sharp decrease in the bearing strength as E/D approaches unity, which indicates that the hole is too close to the specimen edge to adequately support the load. In Figure 7b, there is a sharp decrease in the bearing strength as W/D approaches 2.0, which indicates that the hole is too close to the sides of the specimen to adequately support the load. It is also important to capture the mechanism of failure. Figures 8-12 show typical transition from shear-out mode of failure (E/D = 1.0) to bearing mode of failure (E/D = 4.0) as the edge distance ratio E/D is increased (Figures 8-11) and transition from net-tension mode of failure to bearing mode (Figures 12 and 13) takes place.

The change in mechanism of failure helps to explain why there are transition regions in the graphs of Figure 7a at E/D = 1.0 to 2.0 and Figure 7b at W/D = 2.0 to 3.0. For Figure 7a at low values of E/D, the failure mechanism is shear-out which is a weak type of failure and at high values of E/D,

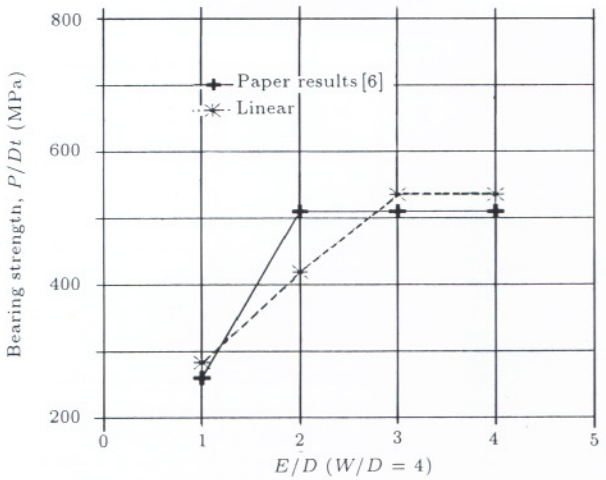

Figure 7a. Variation of ultimate strength of a $[0/90]_s$, cross-ply laminate, W/D = constant, $E/D = 1$ to 4 ($T300/976$).

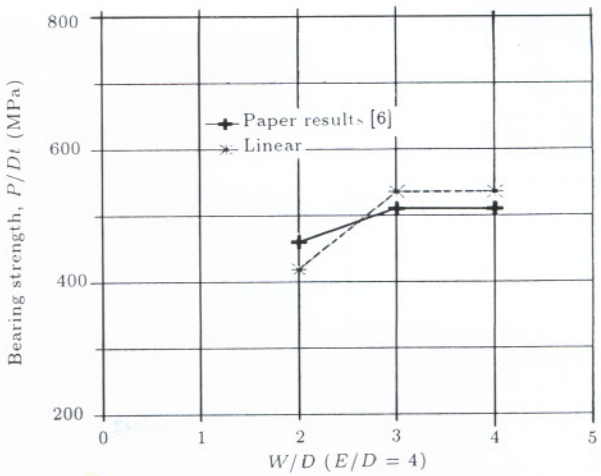

Figure 7b. Variation of ultimate strength of a $[0/90]_s$, cross-ply laminate, E/D = constant, $W/D = 2$ to 4 ($T300/976$).

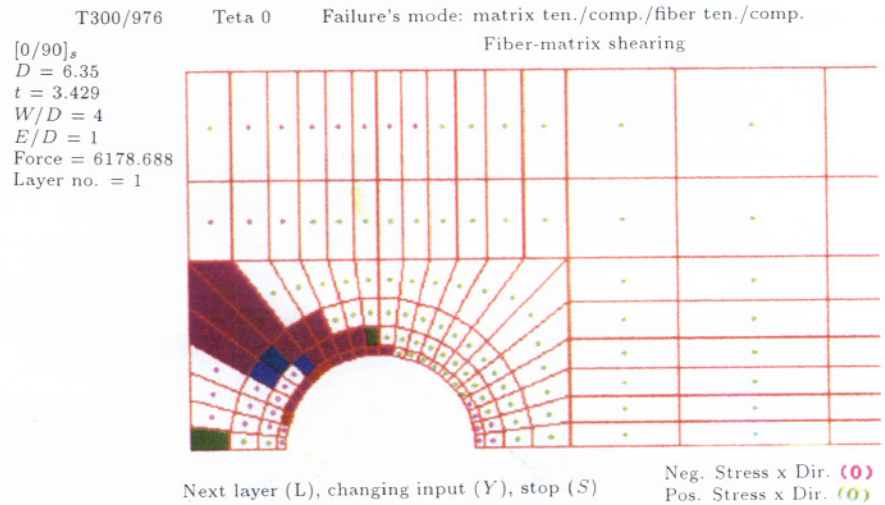

(a)

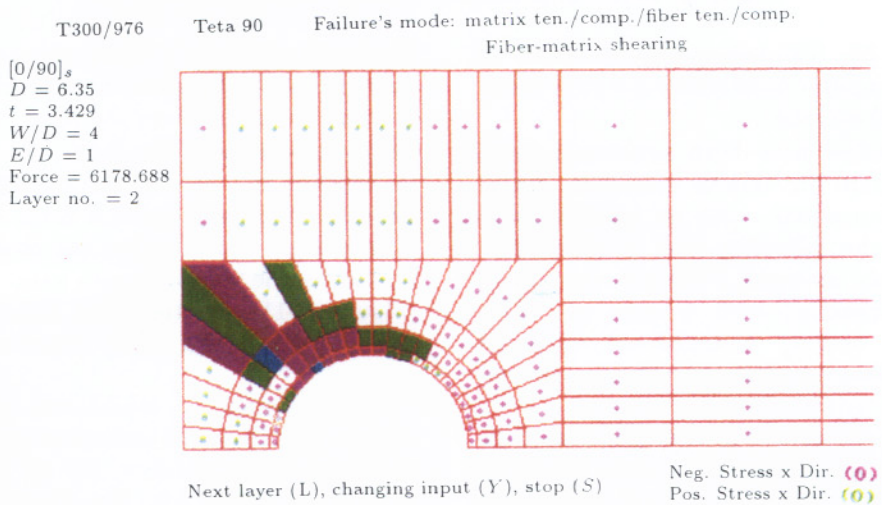

(b)

Figure 8. Shear-out failure mode, [0/90], $t = 3.429$, $W/D = 4$, $E/D = 1$, Force =6178.688.

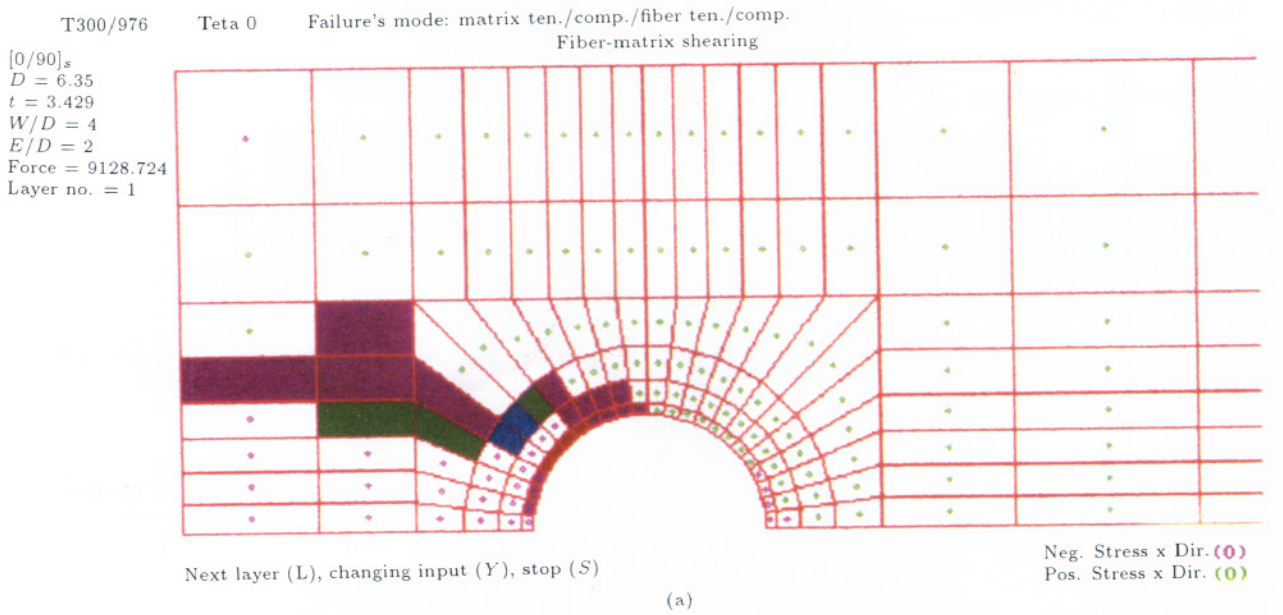

(a)

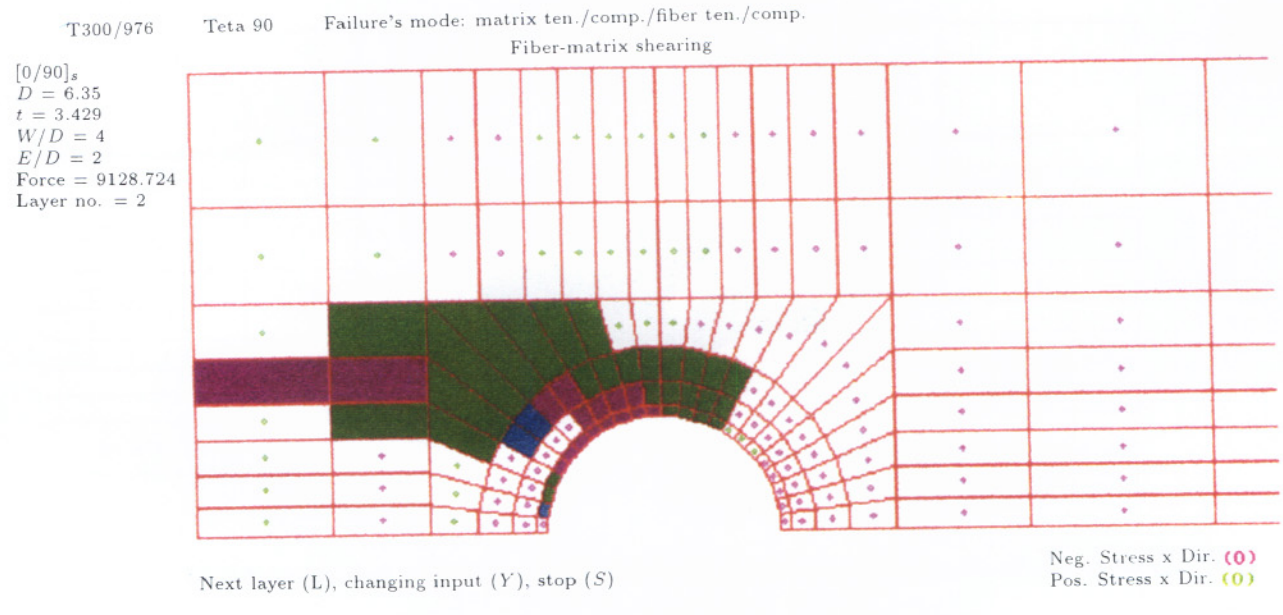

(b)

Figure 9. Transition failure mode, [0/90], $t = 3.429$, $W/D = 4$, $E/D = 2$, Force =9128.724.

the failure mechanism is bearing which is a better method of resisting load. For Figure 7b at low values of W/D, the failure mechanism is net-tension mode and at high values of W/D, the failure mechanism is bearing.

NONLINEAR 2-D MODELING

When the structure is damaged in a region, the assumption of linear behavior, at least in that region, is no longer valid. Therefore, the nonlinear behavior should somehow be taken into account. It must be mentioned that the failure criterion implemented in the linear part of the analysis have actually made the problem piecewise nonlinear. Here, only the nonlinear material behavior is implemented and not the nonlinearities in the large deformation analysis.

NONLINEAR MATERIAL BEHAVIOR MODELING

Fiber-reinforced organic matrix composite materials exhibit material nonlinearity, primarily in the shear-stress/shear-strain relationship of each unidirectional layer [18]. The other single layer material properties tend to remain linear over the elastic range. This is to

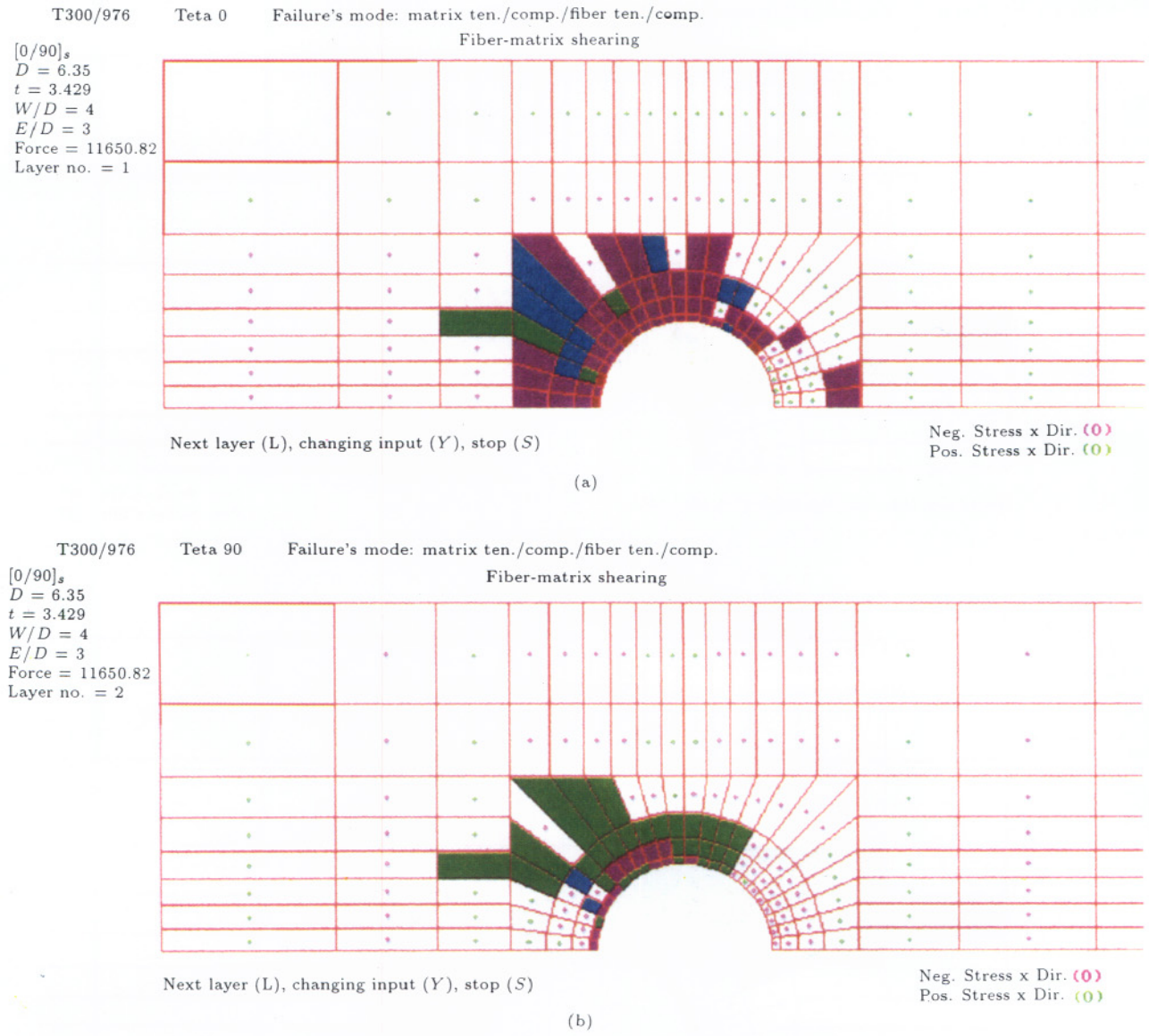

Figure 10. Bearing failure mode, [0/90], $t = 3.429$, $W/D = 4$, $E/D = 3$, Force =11650.82.

and Poisson's ratios ν_x and ν_y behave linearly before failure, while shear modulus G_{xy} is very nonlinear in the elastic range. The nonlinear behavior is introduced in the play level. In plane stress the stress-strain relations in each ply may be expressed as:

$$\begin{Bmatrix} \sigma_x \\ \sigma_y \end{Bmatrix} = \begin{bmatrix} C_{xx} & C_{xy} \\ C_{xy} & C_{yy} \end{bmatrix} \begin{Bmatrix} E_x \\ E_y \end{Bmatrix} \text{ with } \sigma_{xy} = f(\gamma_{xy}) \ , \tag{15}$$

where x and y are coordinates parallel and normal to the fibers, respectively, and C is the reduced stiffness matrix. The function f shows a relationship between the shear stress and shear strain. Different functions have been introduced in this regard (see for example [18-20]). Here, the nonlinear shear-stress/shear-strain relation advanced by Hahn [18] is chosen. Accordingly:

$$\gamma_{xy} = \frac{1}{G_{xy}} \sigma_{xy} + \alpha \sigma_{xy}^3 \ , \tag{16}$$

where G_{xy} is the initial ply shear modulus and α is a constant that has to be determined experimentally. The tangent shear modulus, G_t, defined as the slope of the shear stress versus shear strain at each current position is determined according to:

$$G_t = \frac{d\sigma_{xy}}{d\gamma_{xy}} = \frac{1}{\frac{1}{G_{xy}} + 3\alpha \ \sigma_{xy}^2} . \tag{17}$$

Modified Nonlinear Failure Criteria

The failure criterion which was introduced in the linear part of this analysis would be enhanced by adding

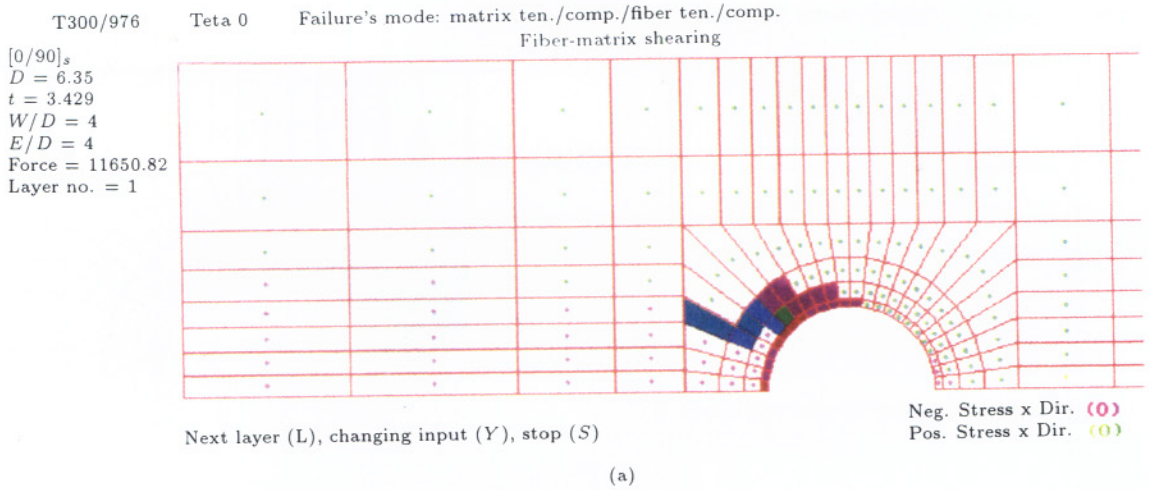

(a)

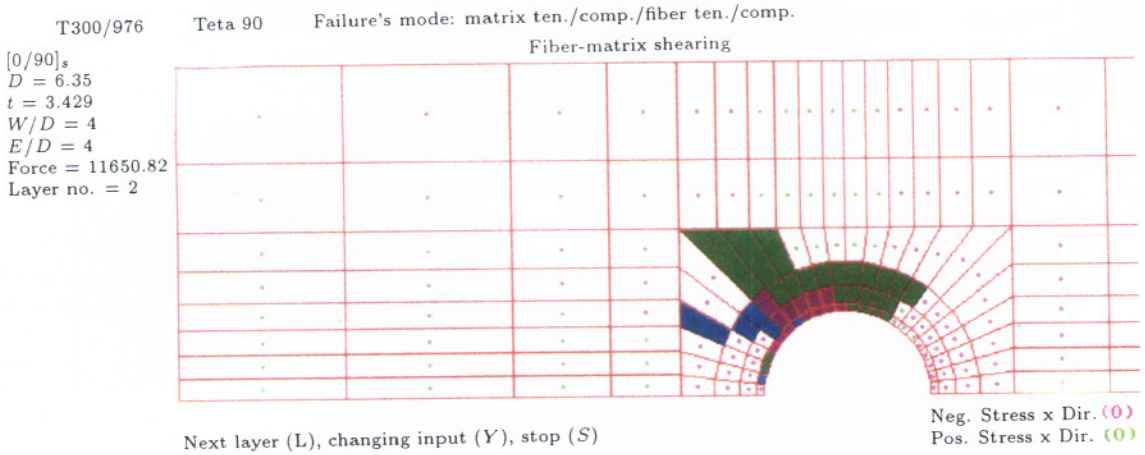

(b)

Figure 11. Bearing failure mode, [0/90], $t = 3.429$, $W/D = 4$, $E/D = 4$, Force =11650.82.

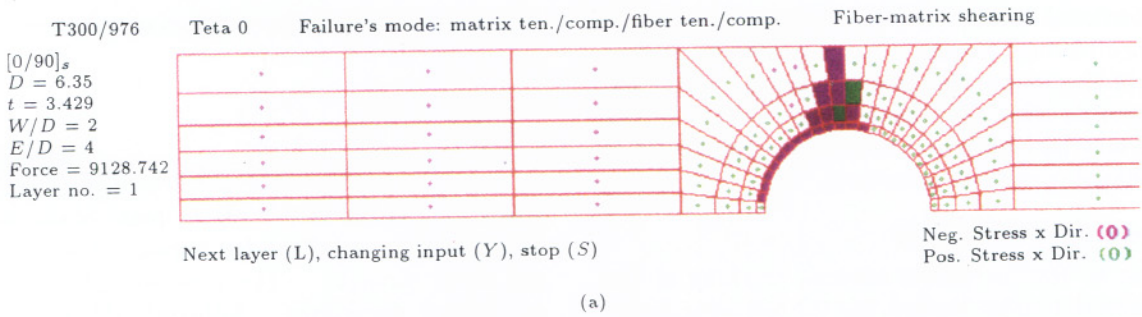

(a)

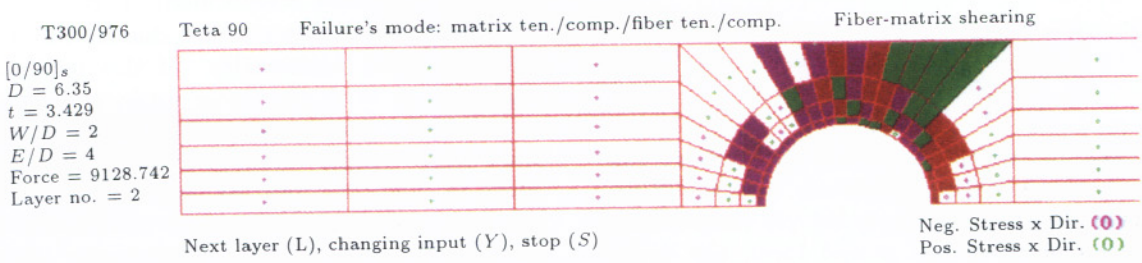

(b)

Figure 12. Net-tension failure mode, [0/90], $t = 3.429$, $W/D = 4$, $E/D = 4$, Force =9128.742.

6-2

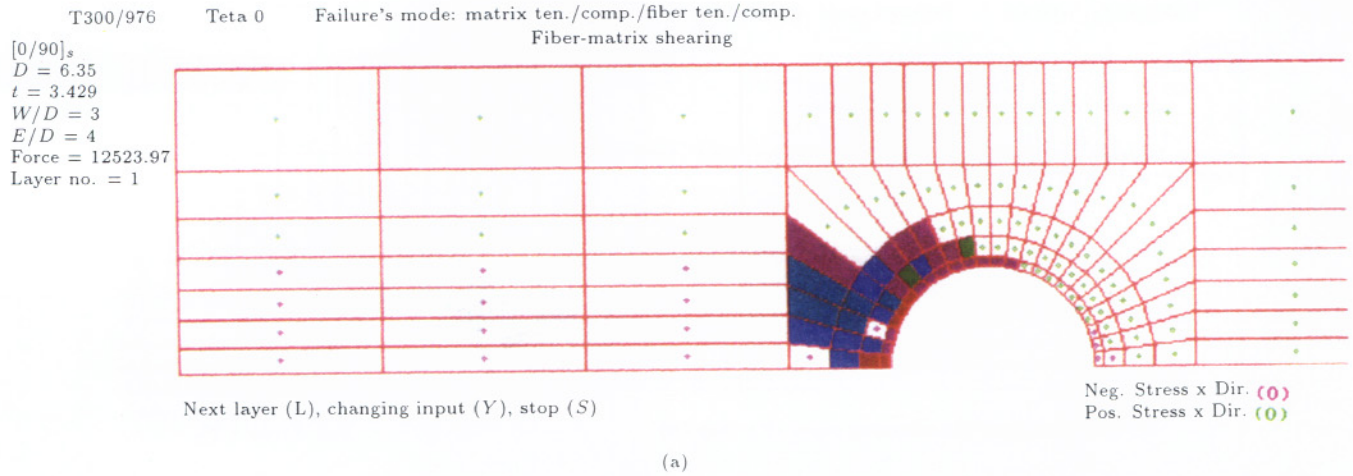

(a)

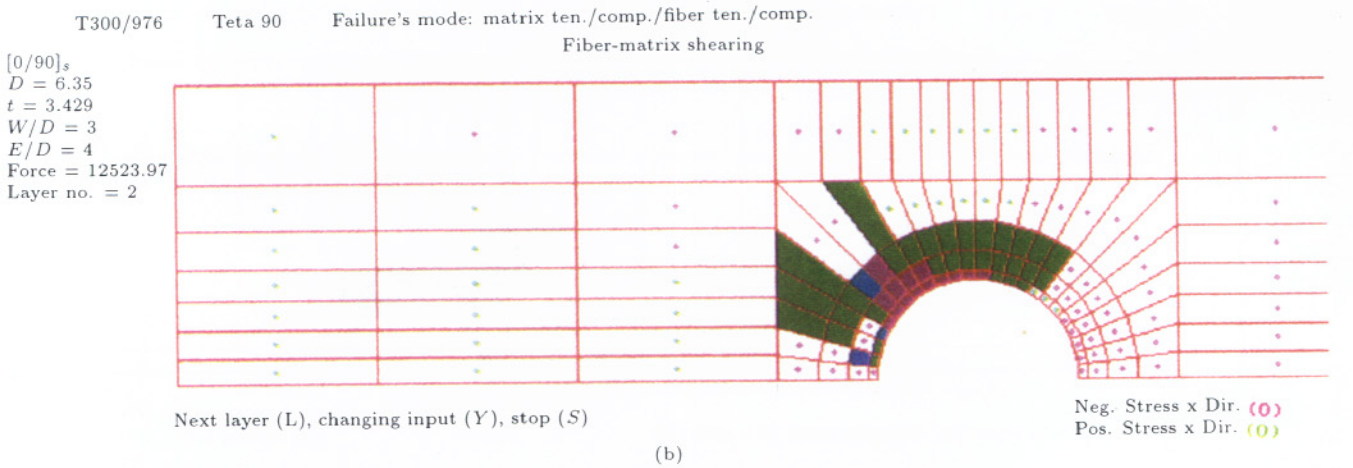

(b)

Figure 13. Bearing failure mode, [0/90], $t = 3.429$, $W/D = 3$, $E/D = 4$, Force =12523.97.

some additional terms. These additional terms are determined through finding a strain energy equivalent to that of the linear case which must be calculated by integrating over the strain range. This failure criterion may be employed to determine the failure of the laminated composite structures.

Nonlinear Matrix Failure

According to Hashin failure criteria, cracking of the matrix material under tension has the following form:

$$\left(\frac{\sigma_y}{S_t}\right)^2 + \frac{\int_0^{\gamma_{xy}} \sigma_{xy} d\gamma_{xy}}{\int_0^{\gamma_{xy}^u} \sigma_{xy} d\gamma_{xy}} > 1 \text{ subjected to } \sigma_y > 0 \,, \tag{18}$$

where σ_y and σ_{xy} are the transverse tensile stress and shear stress in each layer, respectively. S_t is the transverse tensile strength and γ_{xy} is the ply shear-strain. In the denominator of the second term, the upper limit of integration is the ply ultimate shear-strain. By introducing the ply, the shear-stress/shear-strain relationship of the failure criteria may be expressed as:

$$\left(\frac{\sigma_y}{S_t}\right)^2 + \frac{\frac{\sigma_{xy}^2}{2G_{xy}} + \frac{3}{4}\alpha\sigma_{xy}^4}{\frac{S_s^2}{2G_{xy}} + \frac{3}{4}\alpha S_s^4} > 1 \,, \tag{19}$$

where G_{xy} is the initial ply in plane shear modulus, α is the shear nonlinearity parameter and S_s is the ply shear strength. The remaining parameters are as defined previously. Although the expression in this mode appears complicated, it is important to note that the extra terms are due to the definition of the material nonlinearity. If this nonlinearity is weak, i.e., $\alpha \to 0$, the linear forms of failure would be resulted. Similar to matrix tensile failure, the other failure modes criterion may be converted from linear to nonlinear form by just adding the equivalent nonlinear shear stress-strain constitutive formula introduced, so the material nonlinearity affects only the shear-stress/shear-strain terms in their equivalent linear failure criterion. For the sake of brevity, other

modes and their failure criteria are not presented here.

Nonlinear Degradation

Degradation in damaged regions in the nonlinear version is the same as the linear case.

RESULTS OF THE NONLINEAR ANALYSIS

Nonlinear 2-D modeling seeks to improve upon the results of the linear model. Using the 2-D nonlinear computer code, progressive damage simulations were generated. The results of these simulations were compared to the last set of examples of the linear case. The results indicated that they are enhanced in comparison to the work by Lessard and Shokrieh [9] who have employed the same failure criterion.

Nonlinear results improvement is clear and shows that considering nonlinear material behavior is very important. The results of these simulations were also compared to a set of experiments performed using AS4/3501-6 graphite-epoxy composite material [11] (see Table 1 for material properties). The geometries of the samples tested were chosen such that the three possible pinned-joint failure modes could be observed. The geometries correspond to two subgroups of experiments; variation of specimen width and variation of specimen edge distance. For all specimens, the layout was given by $[(45/0/-45/0/90/0/45/0/-45/0)_2]_s$, which is a 40 layer layout containing 4 different ply angles with a dominant amount 0° of plies. Details concerning the experimental method and results can be found in [13]. Figures 14, 15, 16a and 16b summarize the final failure results for the two sets of tests along with predicted values generated from both the linear and nonlinear codes. Each set of data is characterized

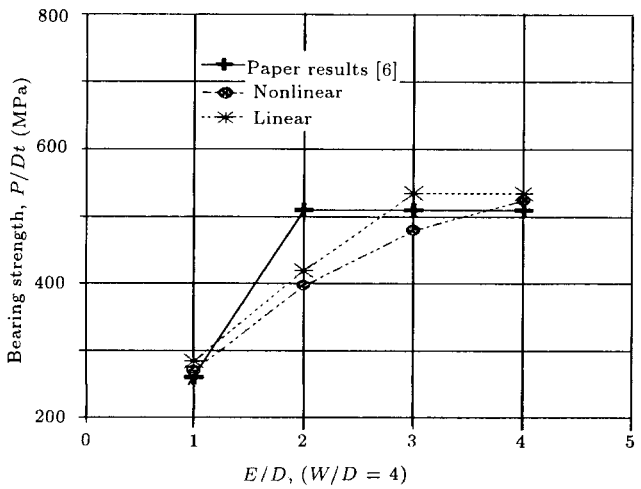

Figure 14. Variation of ultimate strength of a $[0/90]_s$ cross-ply laminate, W/D = constant, E/D= 1 to 4 ($T300/976$).

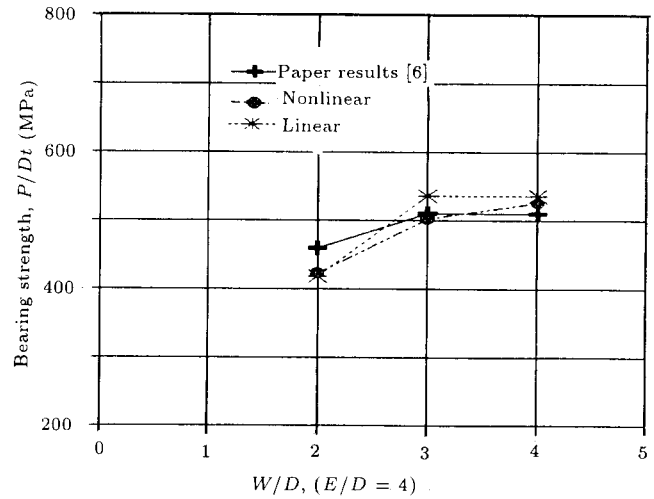

Figure 15. Variation of ultimate strength of a $[0/90]_s$ cross-ply laminate, E/D = constant, W/D = 2 to 4 ($T300/976$).

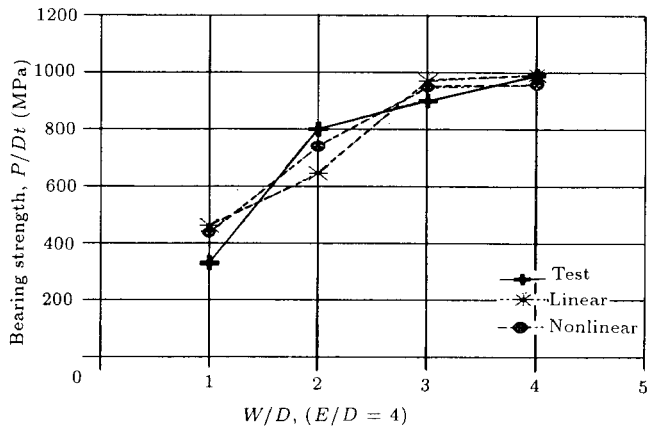

Figure 16a. Variation of ultimate strength (bearing strength) with W/D = constant, E/D= 1 to 4 (AS4/3501-6).

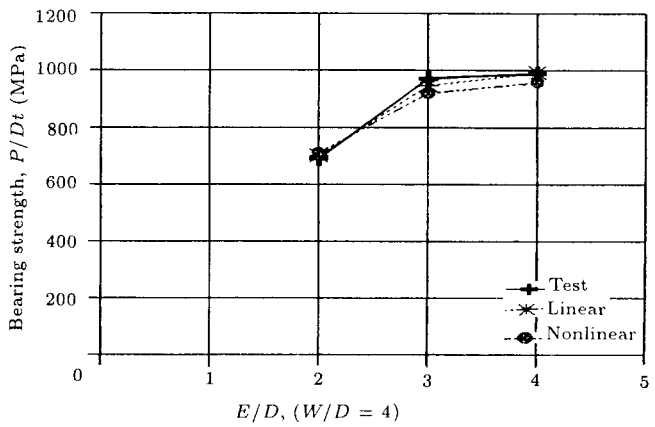

Figure 16b. Variation of ultimate strength (bearing strength) with E/D = constant, W/D= 2 to 4 (AS4/3501-6).

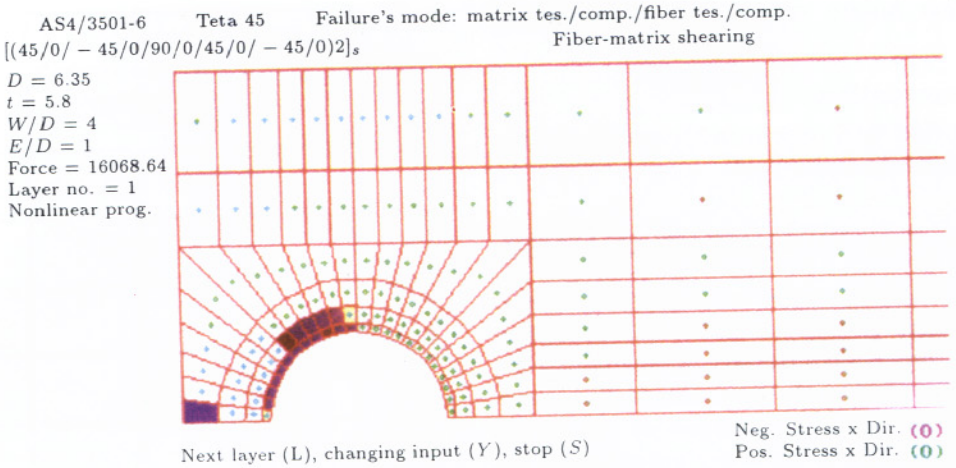

(a)

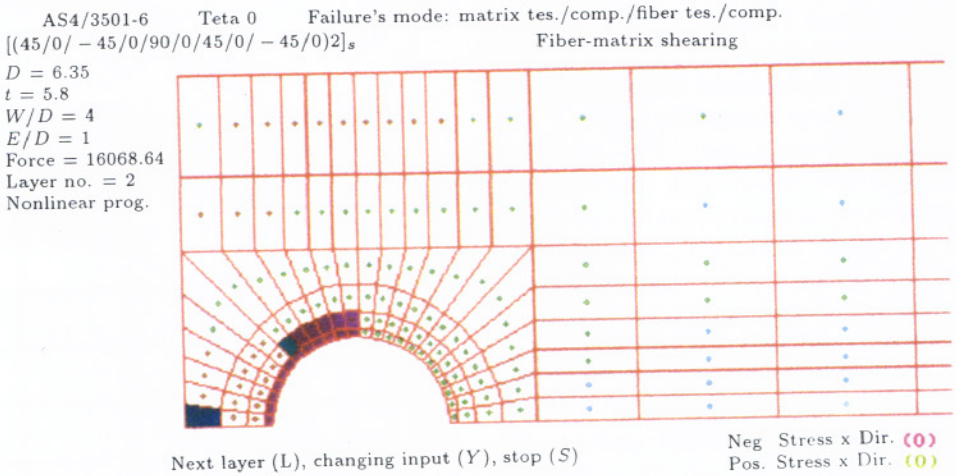

(b)

Figure 17. Shear-out failure mode, [(45/0/-45/0/90/0/45/0/-45/0)2], $t = 5.8$, $W/D = 4$, $E/D = 1$, Force =16068.64.

by weak specimens where the hole is located too close to the sides, $W/D < 3$, or too close to the edge, $E/D < 3$. As the mode changes to the bearing mode of failure, the final failure stress stabilizes and becomes independent of geometry ($W/D > 4$ and $E/D > 4$).

The results show that the nonlinear model predicts very well for data in all ranges, and it is especially promising that the results in the bearing range of failure are close to the experimental values. The linear model gives close results at the lower end of the E/D and W/D scales, indicating that the linear model can capture the shear-out and net-tension mechanism of failure, but not the bearing mechanism. In summary, the nonlinear modeling can predict the failure mode and the ultimate load much better than the linear part of the analysis. A series of figures (Figures 17-20) show the computed results for the prediction of failure mode for AS4/3501-6 using the nonlinear code of analysis. In these figures, the different forms of failure under the increase of loading may be seen.

CONCLUSIONS

A two-dimensional linear and nonlinear analyses of laminated pinned joints are presented. The accuracy and applicability of the algorithm and code are checked. Although the problem in real life is three-dimensional, the results of the two-dimensional problem do compare very well with the experiment and might be employed in a real design. A comparison between linear and nonlinear analyses shows that the results are enhanced by a nonlinear analysis, however, it is very much dependent on the failure criterion, the nonlinear constitutive rule and, also, on the degradation material rule, once a part or a region of the pinned-joint is damaged. A good knowledge of the failure and degradation rules are, thus, a necessity.

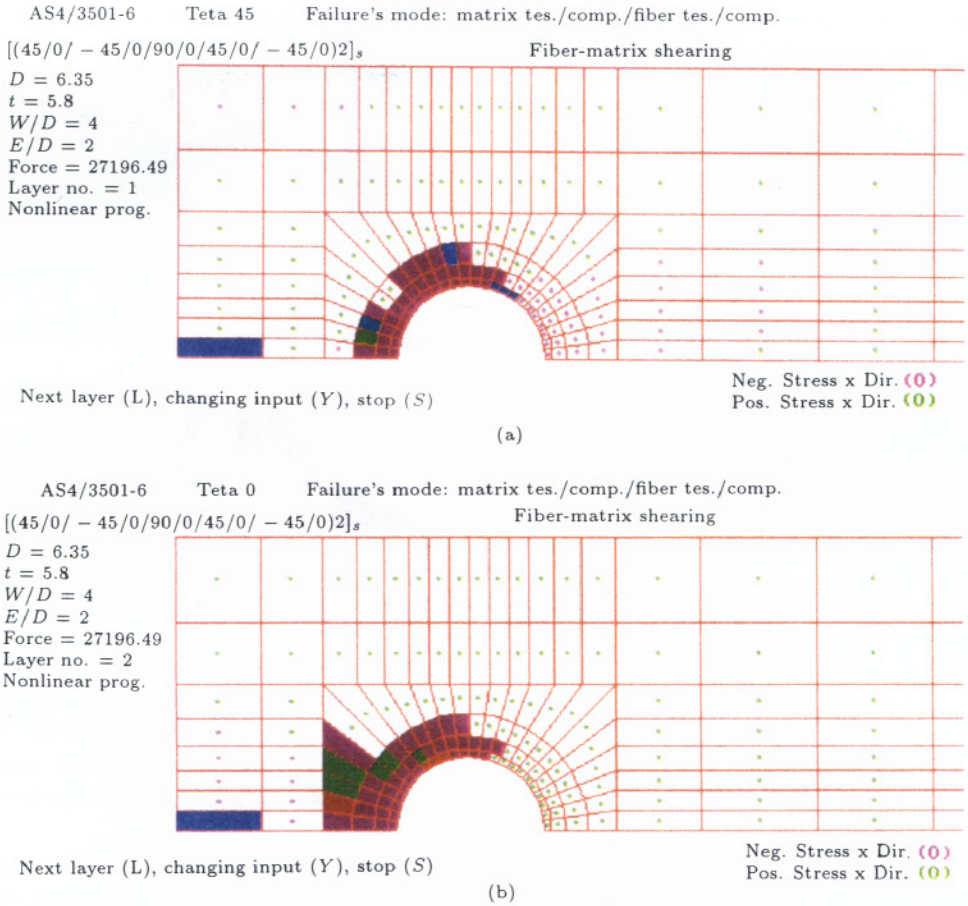

Figure 18. Transition failure mode, [(45/0/-45/0/90/0/45/0/-45/0)2], $t = 5.8$, $W/D = 4$, $E/D = 2$, Force =27196.49.

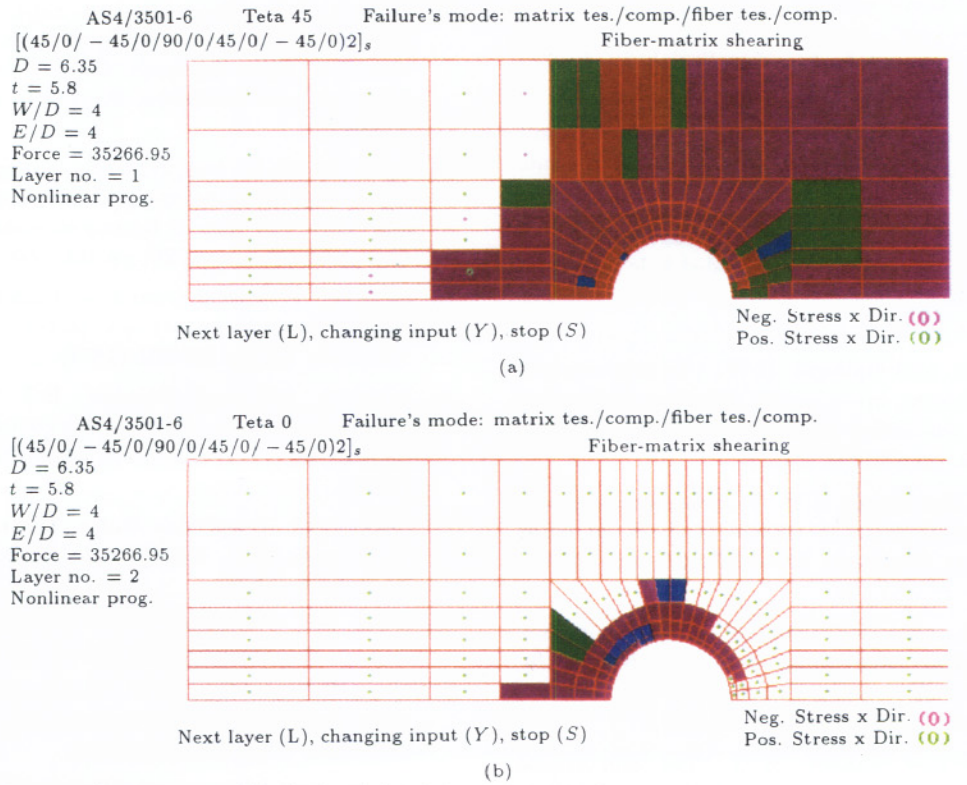

Figure 19. Bearing failure mode, [(45/0/-45/0/90/0/45/0/-45/0)2], $t = 5.8$, $W/D = 4$, $E/D = 4$, Force =35266.95.

6-2

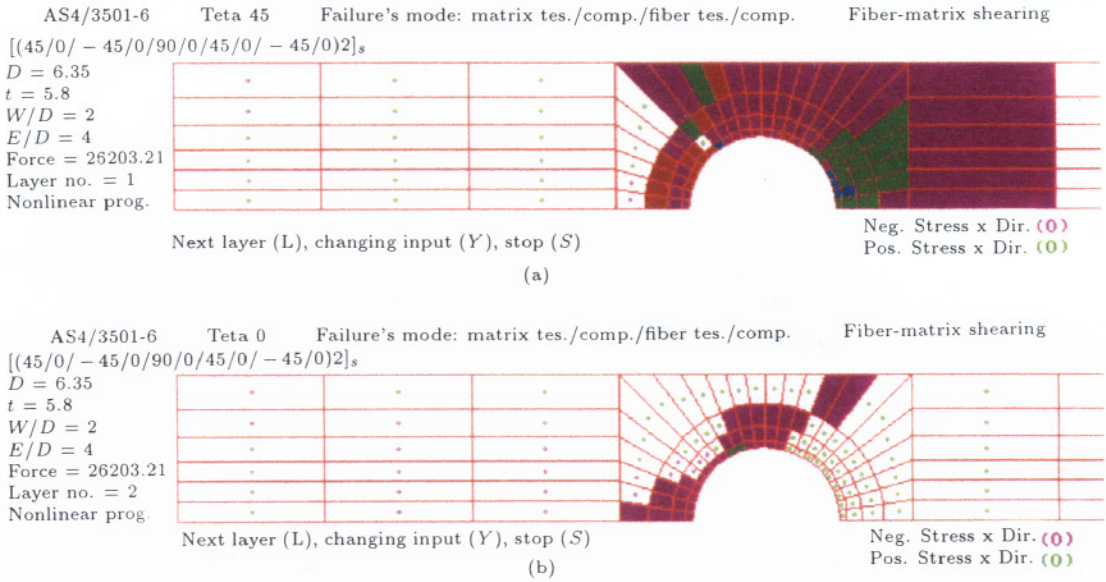

Figure 20. Net-tension failure mode, [(45/0/-45/0/90/0/45/0/-45/0)2], $t = 5.8$, $W/D = 2$, $E/D = 2$. Force =26203.21.

REFERENCES

1. Waszczak, J.P. and Cruse, T.A. "Failure mode and strength prediction of anisotropic bolt bearing specimens", *J. of Composite Materials*, **5**, pp 421-425 (1971).
2. Humphris, N.P. "Migration of the point of maximum stress in a laminated composite structure-A stepwise approach", *Symposium: Joining in Fiber Reinforced Plastics*, Imperial College, London, pp 79-86 (Sept. 14-16, 1978).
3. Soni, S.R. "Failure analysis of composite laminated with a fastener hole", *J. of Composite Materials, ASTM STP*, K.T. Kedward, Ed., American Society for Testing and Materials, pp 145-164 (1981).
4. Tsiang, T.H. and Mandell, J.F. "Damage development in bolt bearing of composite laminates", *AIAA Journal*, **23**, pp 1570-1577 (1985).
5. Conti, P. "Influence of geometric parameters on the stress distribution around a pin-loaded hole in a composite laminate", *Composite Science and Technology*, **25**, pp 83-101 (1986).
6. Serabian, S.M. and Oplinger, D.W. "An experimental and finite element investigation into the mechanical response of pin-loaded laminates", *J. of Composite Materials*, **21**, pp 631-649 (1987).
7. Chang, F.K. and Chang, K.Y. "Post-failure analysis of bolted composite joints in tension or shear-out mode failure", *J. of Composite Materials*, **21**, pp 809-833 (1987).
8. Lessard, L.B. "Bearing failure of composite pinned joints using progressive damage modeling", *ICCM/, International Conference on Composite Materials*, Honolulu, HI, pp 9E1-9E10 (July 15-19, 1991).
9. Lessard, L.B. and Shokrieh, M.M. "Two dimensional modeling of composite pinned-joint failure", *J. of Composite Materials*, **29**, pp 29, 671-697 (1995).
10. Nahas, M.N. "Survey of failure and post-failure theories of laminated fiber-reinforced composites", *J. of Composites Technology& Research*, **8**, pp 138-153 (1986).
11. Hashin, Z. "Failure criteria for unidirectional fiber composites", *J. of Applied Mechanics*, **47**, pp 329-334 (1980).
12. Chang, F.K. and Lessard, L.B. "Damage tolerance of laminated composites containing an open hole and subjected to compressive loadings: Part I-analysis", *J. of Composite Materials*, **25**, pp 2-43 (1991).
13. Lessard, L.B., Poon, C. and Fahr, A. "Composite pinned joint failure modes under progressive damage", *ECCM-V Fifth European Conference on Composite Materials and Exhibition*, Bordeaux, France (April 7-10 1992).
14. Iqbal Shahid, B., Sun, H.T. and Chang, F.K. "Predicting scaling effect on the notched strength of preperg and fiber tow-placed laminated composites", *J. of Composite Materials*, **29**, pp 1063-1095 (1995).
15. De Jong, T. "Stress around pin-loaded holes in elastically orthotropic or isotropic plates", *J. of Composite Materials*, **11**, pp 313-331 (1977).
16. Whitney, J.M. and Nuismer, R.J. "Stress fracture criteria for laminated composites containing stress concentrations", *J. of Composite Materials*, **8**, pp 253-265 (1974).
17. Lekhnitskii, *Anisotropic Plates, Trans.*, S.W. Tsai and T. Cheron, Eds., Gordon and Breach Science, New York, USA (1968).
18. Hahn, H.T. "Nonlinear behavior of laminated composite", *J. of Composite Materials*, **7**, pp 257-271 (1973).
19. Hahn, H.T. and Tsai, S.W. "Nonlinear elastic behavior of unidirectional composite laminate", *J. of Composite Materials*, **7**, pp 102-110 (1973).
20. Sandhu, R.S., Ultimate Strength Analysis of Symmetric Laminates, AFFDL-TR-73-137 (1974).